

Contents lists available at ScienceDirect

Chemical Physics

journal homepage: www.elsevier.com/locate/chemphys



Vibrational contributions to the second-order nonlinear optical properties of π -conjugated structure acetoacetanilide

C. Ravikumar, I. Hubert Joe*, D. Sajan 1

Centre for Molecular and Biophysics Research, Department of Physics, Mar Ivanios College, Thiruvananthapuram-695 015, Kerala, India

ARTICLE INFO

Article history: Received 13 November 2009 In final form 27 January 2010 Available online 1 February 2010

Keywords:
DFT
Normal coordinate analysis
Charge transfer
NBO
Conjugation
Hyperpolarizability

ABSTRACT

FT-Raman and IR spectra of the nonlinear optic (NLO) crystal, acetoacetanilide have been recorded and analyzed. The detailed interpretation of the vibrational spectra has been carried out with the aid of normal coordinate analysis (NCA) following the scaled quantum mechanical force field methodology. The various intramolecular interactions that is responsible for the stabilization of the molecule was revealed by natural bond orbital analysis. The Kurtz and Perry powder reflection technique appeared to be very effective in studies of second-order nonlinear optical properties of the molecule.

© 2010 Elsevier B.V. All rights reserved.

1. Introduction

Recent results suggest that organic materials have drawn substantial interest as potential candidates for applications in electro-optic and photonic devices, such as digital optical switches, light modulators, logic gates and high density optical data storage devices [1,2]. Extensive experimental and theoretical investigations of conjugated organic materials exhibiting large optical nonlinearities have been reported [3,4]. Molecular structure, vibrational spectra and nonlinear optical properties of some acetanilide derivatives have been studied earlier [5–7]. Vijayan et al. [8] reported the growth and characterization of nonlinear optical (NLO) single crystal acetoacetanilide.

Quantum chemical computations are very efficient tool for designing chromophores with improving dipole moments and molecular hyperpolarizabilities [9–11]. It was determined that molecular hyperpolarizability increases with the π -electron conjugation length of the chromophore. The present work deals with FTIR and NIR-FT-Raman spectral study of the organic NLO crystal acetoacetanilide (AAC) to elucidate the correlation between the molecular structure and NLO property, hydrogen bonding and second-order polarizability of the material supported by using the

2. Materials and methods

2.1. Sample preparation

The title compound acetoacetanilide (98% Aldrich) was purchased from Sigma–Aldrich. Recrystallization of AAC was carried out as suggested by Vijayan et al. [8] by slow evaporation method using acetone as a solvent. Good transparent single crystals have been harvested from the solution within a week.

2.2. IR and Raman measurements

The FT-IR spectrum of AAC was recorded using Perkin Elmer RXI spectrometer in the region 4000–500 cm⁻¹, with samples in the KBr. The resolution of the spectrum is 4 cm⁻¹. The NIR-FT-Raman spectrum of AAC crystal was obtained in the range 3500–10 cm⁻¹ using Bruker RFS 100/S FT-Raman spectrophotometer with a 1064 nm Nd: YAG laser source of 100 mW power. Liquid nitrogen cooled Ge-diode was used as a detector. Spectra were collected for samples with 1000 scan accumulated for over 30 min duration. The spectral resolution after apodization was 2 cm⁻¹.

2.3. Second harmonic generation (SHG) analysis

The SHG efficiency of the microcrystalline powders of AAC was examined by the powder reflection technique of Kurtz and Perry

scaled quantum mechanical (SQM) force field technique based on density functional theory (DFT). $\label{eq:condition} % \begin{center} \beg$

^{*} Corresponding author. Tel.: +91 471 2531053; fax: +91 471 2530023. *E-mail addresses*: hubertjoe@gmail.com, hubertjoe@sancharnet.in (I. Hubert Joe).

¹ Permanent address: Department of Physics, Bishop Moore College, Mavelikara, Alappuzha-690 110, Kerala, India.

[12]. Particle size (r), 150 < r < 180 μ m, graded using standard sieve was used for the measurement. Laser beam from Nd:YAG pulsed laser (1064 nm, 15 ns) was used. In the experimental set-up used for the SHG, the incident beam was spilt into 95:5 ratio. The 95% fundamental was focused on the polycrystalline sample, while the 5% of intensity of the fundamental beam was used as a reference beam to normalize the fluctuations of the incident laser. The second harmonic (SH) radiation at 532 nm obtained at the output was filtered using a SH separator to remove the fundamental input radiation. SHG was detected by RCA-931A photomultiplier tube (PMT), which is connected to 100 MHz digital storage oscilloscope (DSO). The change in the intensity of the second harmonic as a function of the fundamental was experimentally measured and is shown in Fig. 1. The SHG efficiency of AAC was evaluated to be 0.85 times that of urea.

3. Computational methods

The DFT computations of AAC has been performed using Gaussian '98 program package [13] at the Becke3-Lee-Yang-Parr (B3LYP) level with standard 6-31G basis set. The first hyperpolarizability β was calculated using Hartree Fock (HF) method on the basis of the finite-field approach. Natural bond orbital (NBO) analysis was carried out with version 3.1 included in Gaussian '98 program at the B3LYP/6-31G level of theory. The geometries were fully optimized without any constraint with the help of analytical gradient procedure implemented within Gaussian 98W program. The harmonic vibrational wavenumbers have been analytically calculated by taking the second-order derivative of energy using the similar level of theory. Multiple scaling of the force field has been performed by the SQM procedure [14,15] to offset the systematic errors caused by basis set incompleteness, neglect of electron correlation and vibrational anharmonicity [16]. Normal coordinate analysis has been performed to obtain full description of the molecular motion pertaining to the normal modes using the MOL-VIB program version 7.0 written by Sundius [17,18]. The Raman activities (S_i) calculated by Gaussian 98 program have been suitably adjusted by the scaling procedure with MOLVIB and subsequently converted to relative Raman intensities (I_i) using the following relationship derived from the basic theory of Raman scattering [19,20]

$$I_{i} = \frac{f(v_{0} - v_{i})^{4} S_{i}}{v_{i} \left[1 - \exp\left(\frac{-hcv_{i}}{kT}\right)\right]}$$
(1)

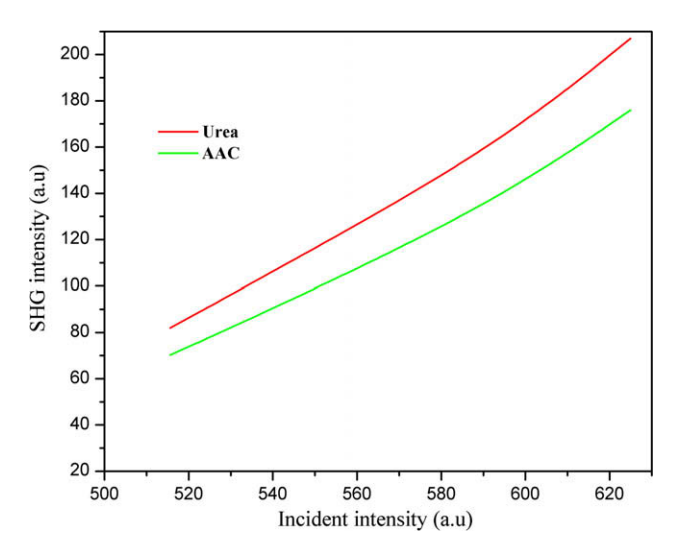


Fig. 1. SHG variation in AAC for the particle size $150 < r < 180 \, \mu m$ as compared to urea.

where v_0 is the exciting frequency (in cm⁻¹ units), v_i is the vibrational wavenumber of the ith normal mode, h, c and k are universal constants, and 'f' is the suitably chosen common scaling factor for all the peak intensities. The simulated IR and Raman spectra have been plotted using pure Lorentzian band shapes with full width at half maximum (FWHM) of 10 cm^{-1} .

The second-order polarizability or first hyperpolarizability β was calculated using HF/6-31G* basis set on the basis of the finite-field approach. The components of the first hyperpolarizability can be calculated using the following equation

$$\beta_i = \beta_{iii} + 1/3 \sum (\beta_{ijj} + \beta_{jij} + \beta_{jji}), \quad (i \neq qj)$$
 (2)

Using the x, y and z components, the magnitude of the first hyperpolarizability tensor can be calculated by

$$\beta = (\beta_x^2 + \beta_y^2 + \beta_z^2)^{1/2} \tag{3}$$

The complete equation for calculating the magnitude of first hyperpolarizability from Gaussian 98W output is given as follows [21]:

$$\beta = [(\beta_{xxx} + \beta_{xyy} + \beta_{xzz})^{2} + (\beta_{yyy} + \beta_{yzz} + \beta_{yxx})^{2} + (\beta_{zzz} + \beta_{zxx} + \beta_{zyy})^{2}]^{1/2}$$
(4)

To calculate the hyperpolarizability, the origin of the Cartesian coordinate system was chosen as the center of mass of the compound [22]. The components of the hyperpolarizability tensor are shown in Table S1 (in Supplementary material). The calculated first hyperpolarizability of AAC is 7.43×10^{-31} esu which is five times that of urea.

4. Results and discussion

4.1. Optimized geometry

The optimized molecular structure of the monomer (Fig. 2) and dimer (Fig. 3) of AAC was calculated using Gaussian 98W program. The selected optimized geometrical parameters are given in Table 1. The molecular structure is non-planar with the dihedral angle between the planes of the aryl ring and the acetyl group is 4.4°. The steric interaction between the phenyl ring and acetyl group is reflected in the angles subtended at the N atom, C₁-N₇- $H_{13} = 116.54$, $C_1 - N_7 - C_{14} = 128.62$ and $H_{13} - N_7 - C_{14} = 114.56^{\circ}$. The shortening of C_1 -N bond (\sim 0.003 Å) from the experimental value is due to the nitrogen atom attached to the benzene ring. Similarly, $N-C_{14}$ bond (1.345 Å) is short compared with the XRD results [23] but it is in agreement with determinations of similar peptide linkages in abundant other compounds [24]. The sum of the bond angles about N₇ is 359.97° (=360°), indicating that this atom is sp^2 hybridized. The intramolecular $H_{12}\!\cdots\!O_{15}$ and $H_{33}\!\cdots\!O_{39}$ distances 2.264 and 2.225 Å (Table S2; in Supplementary material) are significantly shorter than the van der Waals separation between

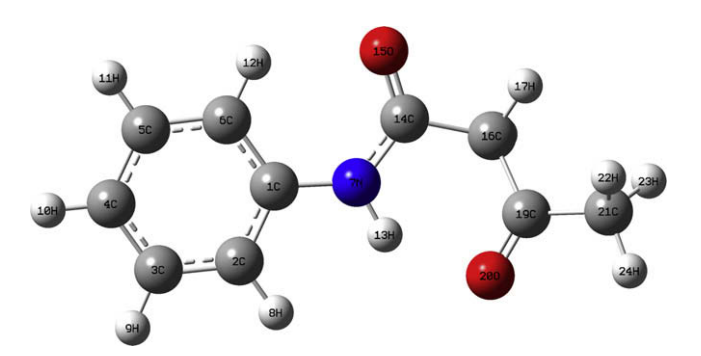


Fig. 2. Optimized structure of AAC calculated at B3LYP/6-31G^{*}.

Download English Version:

https://daneshyari.com/en/article/5375215

Download Persian Version:

https://daneshyari.com/article/5375215

Daneshyari.com